Chinese Physics C

Study on space charge effects of the CSNS/RCS

XU Shou-Yan(许守彦)   WANG Sheng(王生)[1]

Institute of High Energy Physics, Chinese Academy of Sciences, Beijing 100049, China

Abstract: The Rapid Cycling Synchrotron (RCS) is a key component of the China Spallation Neutron Source (CSNS). The space charge effect is one of the most important issues in the CSNS/RCS, which limits the maximum beam intensity, as well as the maximum beam power. Space charge effects are the main source of emittance growth and beam loss in the RCS. Space charge effects have been studied by simulation for the CSNS/RCS. By optimizing the painting orbit, the optimized painting distribution was obtained. The space charge effects during the acceleration are studied and dangerous resonances, which may induce emittance growth and beam loss, are investigated. The results are an important reference for the design and commissioning of the CSNS/RCS.

Key words: space charge, injection, emittance growth, CSNS

PACS: 29.27.Bd   **DOI:** 10.1088/1674-1137/35/12/014

1   Introduction

The China Spallation Neutron Source (CSNS) is an accelerator-based facility. It operates at a 25 Hz repetition rate with an initial design beam power of 100 kW and is capable of being upgraded to 500 kW. The CSNS consists of a 1.6 GeV Rapid Cycling Synchrotron (RCS) and a 80 MeV linac, which can be upgraded to 250 MeV for a beam power upgrade to 500 kW. The RCS accumulates an 80 MeV injected beam, accelerates the beam to the designed energy of 1.6 GeV and extracts the high energy beam to the target [1, 2].

The lattice of the CSNS/RCS is a triplet based four-fold structure. Table 1 shows the main parameters for the lattice and injection.

Due to the high beam density and high repetition rate, the rate of beam loss must be controlled to a very low level. In this kind of high power RCS, especially in the low energy end, the space charge effects can result in emittance growth and halo formation, which may contribute to beam losses. The space charge effect is one of the most important issues of the CSNS/RCS, which limits the maximum beam intensity, as well as the maximum beam power. Much simulation work has been done to study the space charge effects of CSNS/RCS by using ORBIT and SIMPSONS. The simulation results are the foundation of the physical design and the choice of design parameters.

Table 1.   Main parameters of the lattice and injection.

circumference/m	227.92
super period	4
betatron tunes/(h/v)	4.86/4.78
RF harmonics	2
injection energy/MeV	80
accumulated particles per pulse	1.56×10^{13}
linac peak current/mA	13
injection rms emittance/(π mm·mrad)	1.0
β_x/β_y of the injected beam/m	1.7/1.8
α_x/α_y of the injected distribution	0/0
β_x/β_y at the injection point of RCS/m	6.4/5.8
α_x/α_y at the injection point of RCS	0/0
transverse acceptance/(π mm·mrad)	540
painting scheme	Anti-Correlated

ORBIT [3] and SIMPSONS [4] are 3-D particle tracking codes for circular accelerators. A benchmark between ORBIT and SIMPSONS produces excellent agreement by using the SNS lattice [5]. Careful benchmarking between these two codes has also been performed by using the CSNS/RCS lattice. As benchmarking tests, 3-D simulations of the injection using an anti-correlated painting scheme and the acceleration have been done. Table 2 shows the painted emittances without space charge effects obtained by using ORBIT and SIMPSONS, respectively, and Table 3 shows the painted emittances with space charge effects. Without space charge effects, the simulation results by using two codes agree very well. these with

space charge effects, both simulation results by OR-BIT and SIMPSONS show that there are space charge coupling effects during injection, and the painted 99% emittance in the vertical direction is greater than in the horizontal direction because of more halo particles in this direction, in which the emittance is painted from large to small during injection.

Table 2. The painted emittance without space charge effects obtained by the ORBIT and SIMPSONS codes.

	SIMPSONS	ORBIT
horizontal rms emittance/ (π mm·mrad)	61.7	62
vertical rms emittance/ (π mm·mrad)	61.4	60
horizontal 99% emittance/ (π mm·mrad)	237	243
vertical 99% emittance/ (π mm·mrad)	238	244

An initial transverse KV distribution is used in the simulation for benchmarking tests. The initial normalized horizontal and vertical rms emittances are both 30 π mm·mrad. The time evolutions of the normalized rms emittances during acceleration with and without space charge effects obtained by ORBIT and SIMPSONS are shown in Fig. 1. The simulation results agree with each other very well.

Table 3. The painted emittance with space charge effects obtained by the ORBIT and SIMPSONS codes.

	SIMPSONS	ORBIT
horizontal rms emittance/ (π mm·mrad)	64.4	68.8
vertical rms emittance/ (π mm·mrad)	57.8	52
horizontal 99% emittance/ (π mm·mrad)	255	282
vertical 99% emittance/ (π mm·mrad)	294	302

ORBIT can be used to perform 1-D tracking as well as 3-D tracking, and it can read macro-particles from a given file. SIMPSONS is a 3-D tracking program which can be used to study individual particle behavior by tracking test particles. SIMPSONS is used to simulate the transverse phase space painting and optimize the bump function to find the best painted distribution, while ORBIT is used for the initial KV distribution.
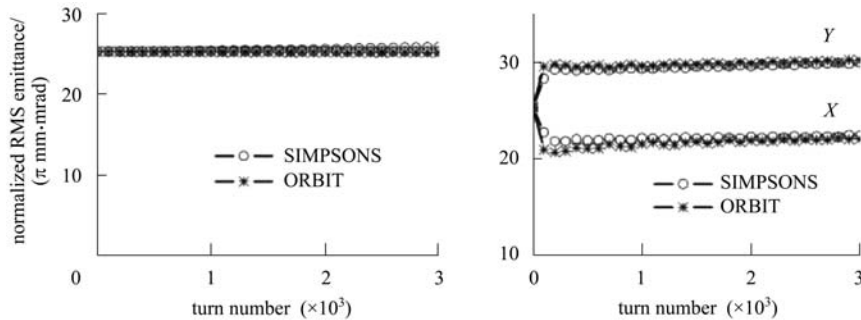

Fig. 1.   The time evolutions of normalized rms emittances during acceleration with (right) and without (left) space charge effects obtained by ORBIT and SIMPSONS.

2   Space charge effects during injection

The CSNS/RCS injection is performed in a long drift space of a straight dispersion-free section [6]. The anti-correlated painting scheme is chosen. Painting is achieved by moving the orbit of the circulating beam at the stripping foil as a function of time (called the bump function) with injection bump magnets in both horizontal and vertical directions, while keeping the injected beam stationary, so the painted beam distribution is determined by the bump function.

In the case of no space charge effects, to obtain a uniform distribution in the transverse phase space with a constant Linac current during the injection, the injection bump orbit should satisfy Eq. (1),

$$\frac{r\mathrm{d}r}{\mathrm{d}t} = c, \qquad (1)$$

where r indicates x or y, c is a constant. For the CSNS/RCS, the emittance is painted from small to large in the horizontal direction, while from large to small in the vertical direction. Eq. (1) leads to

$$\begin{aligned} x(t) &= x_0\sqrt{\frac{t}{t_{\mathrm{inj}}}}, 0 \leqslant t \leqslant t_{\mathrm{inj}} \\ y(t) &= y_0\sqrt{\frac{t_{\mathrm{inj}}-t}{t_{\mathrm{inj}}}}, 0 \leqslant t \leqslant t_{\mathrm{inj}} \end{aligned}, \qquad (2)$$

where t_{inj} is the injection time, x_0 and y_0 are the maximum bumps during injection. Fig. 2 shows the painted beam distribution in the vertical direction by using the bump functions of Eq. (2), under the injection conditions shown in Table 1. It can be observed that due to space charge effects, the beam distribution deviates from the uniform distribution obviously and some halo particles are generated.
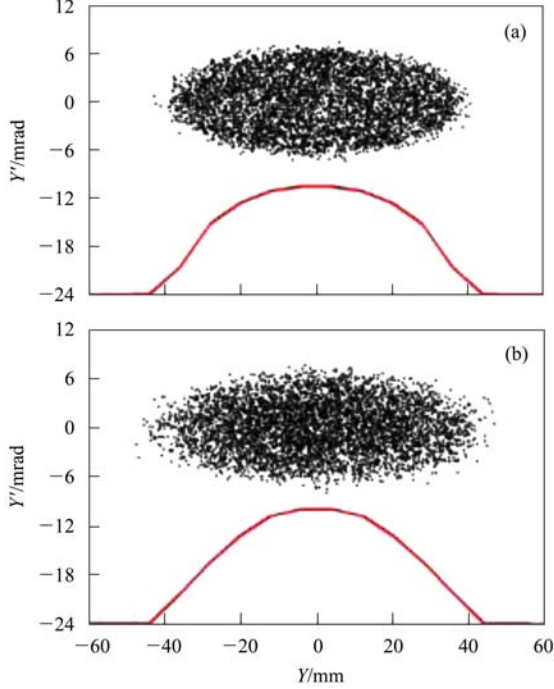

Fig. 2. Beam distributions in vertical phase space at the end of injection without (a) and with (b) space charge effects.

For the unbunched beam with a round transverse uniform distribution up to a radius a, the Lorentz force experienced by a particle is

$$F_r = \frac{2\lambda e^2}{a^2\gamma^2}r \quad r \leqslant a$$
$$\phantom{F_r = \frac{2\lambda e^2}{a^2\gamma^2}r} , \qquad (3)$$
$$F_r = \frac{2\lambda e^2}{r\gamma^2} \quad r > a$$

as shown in Fig. 3(b).

For anti-correlated painting, the beam distribution in real space is not uniform during the injection, as shown in Fig. 4(a), which shows the distribution after 20 turns injection without space charge effects. The Lorentz force experienced by particles with space charge effects is shown in Fig. 4(b), and the Lorentz force drives the particles to move towards the inner and outer region in the vertical phase space, and produce higher intensity in the beam center.
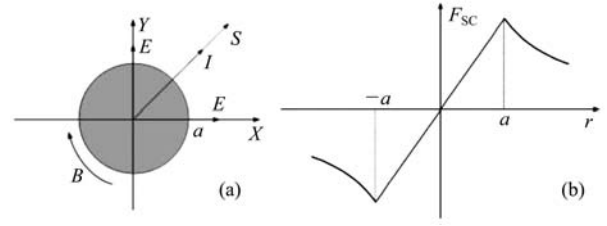

Fig. 3. (a) Electric and magnetic field in a uniform distribution beam; (b) the Lorentz force experienced by particles for the uniform distribution.
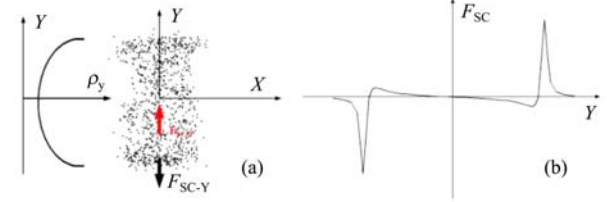

Fig. 4. (a) The distribution in the real space after 20 turns injection without space charge effects; (b) the Lorentz force experienced by particles for the distribution shown in (a).

Some studies of painting orbit optimization have been done for the injection of CSNS/RCS. To reduce halo formation, the exponential function for the vertical bump is adopted at the beginning of the injection [7]. To reduce the center intensity of the painting beam, similar to SNS [8], a hollow anti-correlated painting scheme is adopted [9]. These efforts all benefit the painting beam distribution of the CSNS/RCS.

To produce a much more uniform distribution with space charge effects and reduce halo production, a more general bump function is suggested. Aiming at injecting less particles in the inner and outer region of the phase space, Eq. (1) is modified as

$$\frac{y\mathrm{d}y}{\mathrm{d}t} = c|t - t_{mid}|^n, \quad 0 < n < 1 \qquad (4)$$

then one can get bump functions as [10]

$$y = \sqrt{y_{mid}^2 + \frac{y_{max}^2 - y_{mid}^2}{(t_{inj} - t_{mid})^{n+1}}(t_{mid} - t)^{n+1}},$$
$$0 < t < t_{mid}$$
$$\phantom{y = \sqrt{y_{mid}^2}} , \qquad (5)$$
$$y = \sqrt{y_{mid}^2 - \frac{y_{mid}^2 - y_{min}^2}{t_{mid}^{n+1}}(t - t_{mid})^{n+1}},$$
$$t_{mid} < t < t_{inj}$$

where $y_{max} < y_0$, $y_{min} > 0$ are the maximum and minimum bumps during injection, y_{mid} is a certain bump position during injection, t_{mid} is the time which

corresponds to bump $y_{\mathrm{mid},}$, and $y_{\mathrm{mid},}$, n is determined by simulation. For CSNS/RCS $y_{\mathrm{mid}} = y_0/2$, $n=1/2$ are adopted after optimizations. Fig. 5 shows 1-D density profiles in the vertical direction for different bump functions. The distribution in the vertical phase space painted with the new bump functions described in Eq. (5) is more uniform than the distribution painted with bump functions described by Eq. (2).
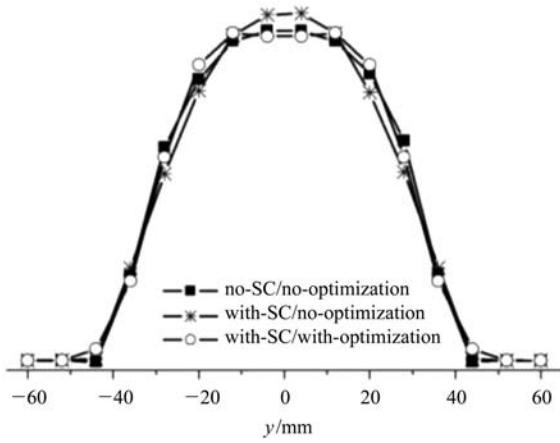

Fig. 5.   1-D density in vertical direction. x-axis: beam size in mm; y-axis: density in arbitrary units.

3   Space charge effects during acceleration

To study the space charge effects during the acceleration in a cycle, two initial transverse beam distributions are employed, one is the KV distribution, and the other is the painted distribution by using optimized bump functions.

For the initial KV distribution with the unnormalized rms emittances of 60 π mm·mrad in both horizontal and vertical directions, Fig. 6(a) shows the time evolution of unnormalized rms emittances. There is strong transverse coupling induced by the space charge. Space charge may lead to emittance exchange through space charge coupling in high current synchrotrons. Space charge coupling is an internal resonance driven by the self-consistent space charge potential of coherent eigenmodes [11, 12]. Fig. 6(c) shows the fourth-order model, which has the space charge potential of x^2y^2, already developed by 200 turns [13]. The working point (4.86, 4.78) is close to the resonance $2v_x-2v_y=0$, which is driven by the fourth order coupling term x^2y^2 in the Hamiltonian. The emittance exchange is probably caused by the resonance $2v_x-2v_y=0$.
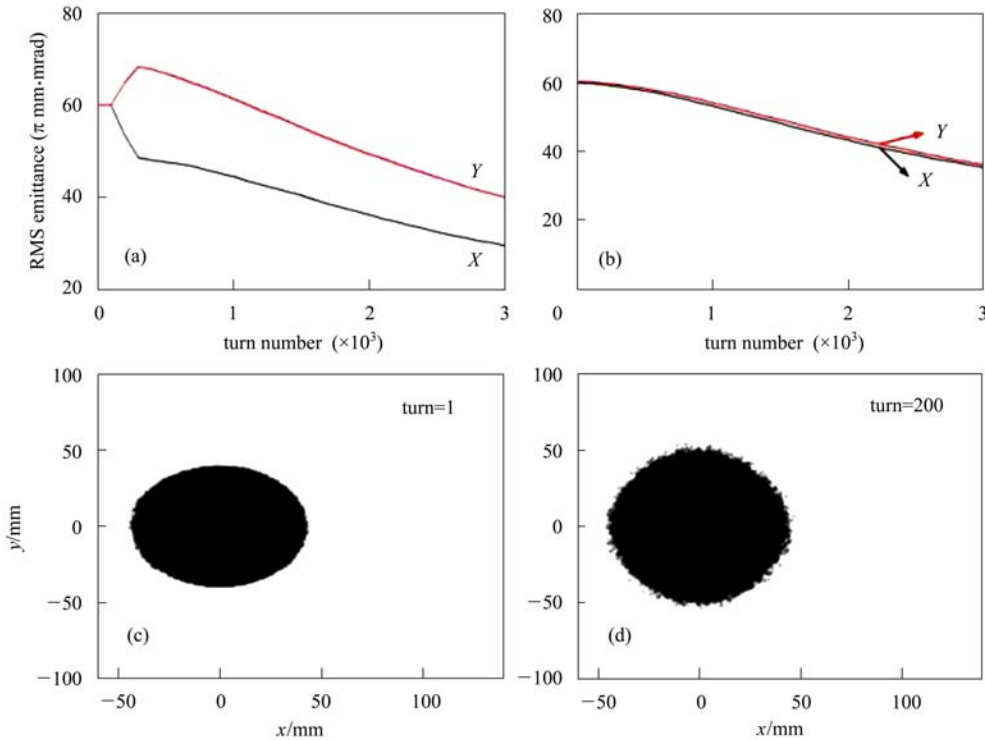

Fig. 6.   (a) The time evolution of unnormalized rms emittances at the early stage for a tune of (4.86, 4.78); (b) the time evolution of unnormalized rms emittances at the early stage for a tune of (5.82, 4.80); (c) beam distribution in (x, y) real space at the first turn for a tune of (4.86, 4.78); (d) beam distribution in (x, y) real space at the 200th turn for a tune of (4.86, 4.78).

The resonance $2v_x-2v_y=0$ was first analyzed by Montague [14]. This resonance can occur even for a linear lattice without any perturbations since it requires only a zero harmonic in the Fourier component of the density perturbation. Due to the fact that this resonance is a difference resonance, such coupling can lead to a significant effect for a beam with unequal emittances [14, 15]. The perfect KV distribution has no coupling. Small density fluctuations in the numerically generated initial KV distribution and different beam parameters resulting from the rms matching procedure may lead to an exponential growth of the eigenmode with the potential of x^2y^2, which is capable of exciting the Montague resonance [11, 16]. The Montague resonance can be avoided by sufficient splitting of the tunes. As shown in Fig. 6 (b), for a tune of (5.82, 4.80), there is no coupling resonance found.

Figure 7 shows the simulation results with painted distribution obtained by anti-correlated painting. Unlike the results obtained using KV distribution, there is no great rms emittance exchange and no high-order collective beam mode is observed. The explanation might be that in the painted beam, a finite spread of single particle frequencies leads to Landau damping and suppression of instabilities for some modes [11–13].

In the simulations with painted distribution, diffusion of particles among different parts in the phase space occurs during acceleration, as shown in Fig. 8. In order to study the mechanisms, 30 test particles are set in the simulations by SIMPSONS. The test particles are chosen to cover the entire region of interest. At the injection point, the position of a test particle in the phase space is recorded turn by turn, and the Poincaré map is obtained. The Poincaré maps of most test particles are distorted during acceleration. For test particle A, the time evolution of the Courant-Snyder (C-S) invariant is shown in Fig. 9, and space charge coupling resonance seems to be excited. For test particles B/C/D the resonance $3v_x=14$ is probably excited. The dynamic feature of test particle E is complicated, and the time evolution of the C-S invariant is shown in Fig. 9. Fig. 10 shows the Poincaré maps in the horizontal direction during 625–649 turns and in the vertical direction during 637–652 turns of test particle E. The horizontal C-S invariant growth during 57–74 turns is probably caused by the resonance $3v_x=14$, and during 625–649 turns by $5v_x=23$. During 637–652 turns the resonance $2v_y=9$ is probably excited, which results in the vertical C-S invariant growth.
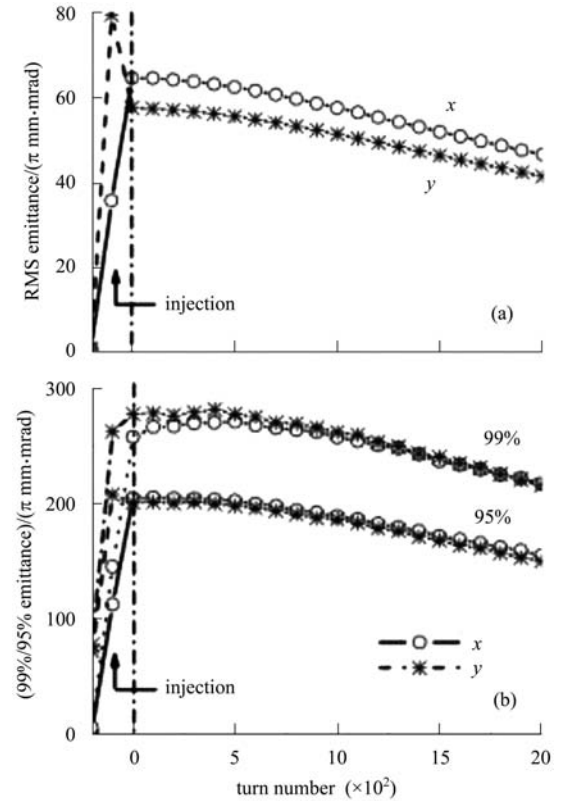

Fig. 7.   The time evolution of the unnormalized emittances at the early stage. (a) rms emittance; (b) 99% emittance.
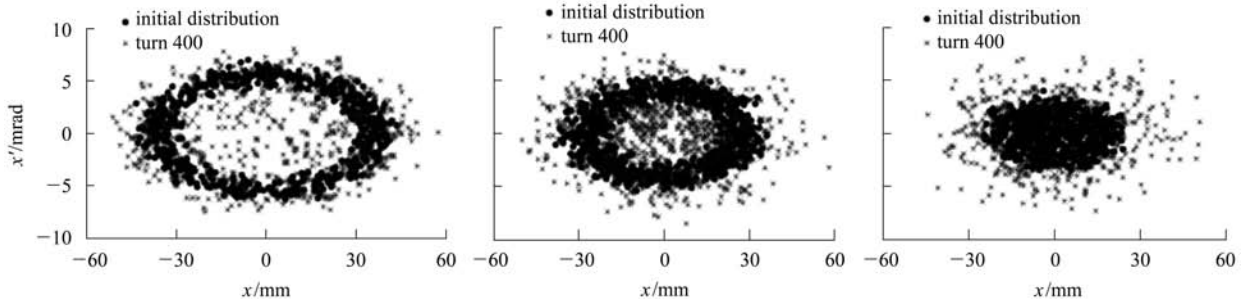

Fig. 8.   Diffusion of particles among different parts in the phase space during acceleration: particles in the outer region (left); particles in the middle region (middle); particles in the inner region (right).
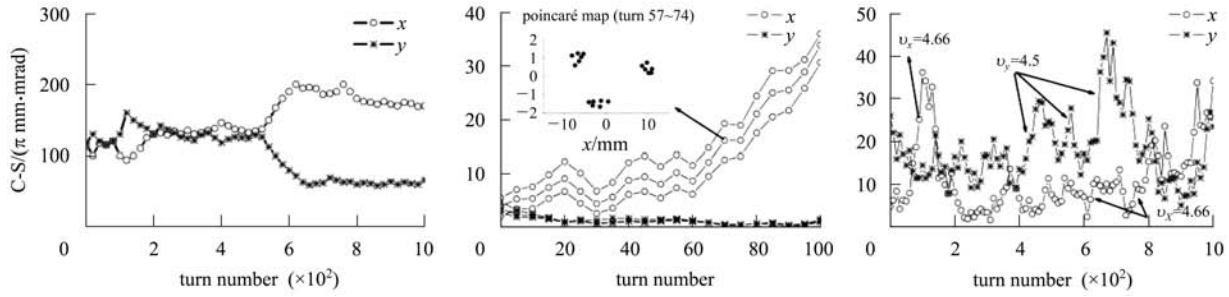
Fig. 9.   The time evolution of the C-S invariant of test particle A (left), test particles B/C/D (middle), and test particle E (right).
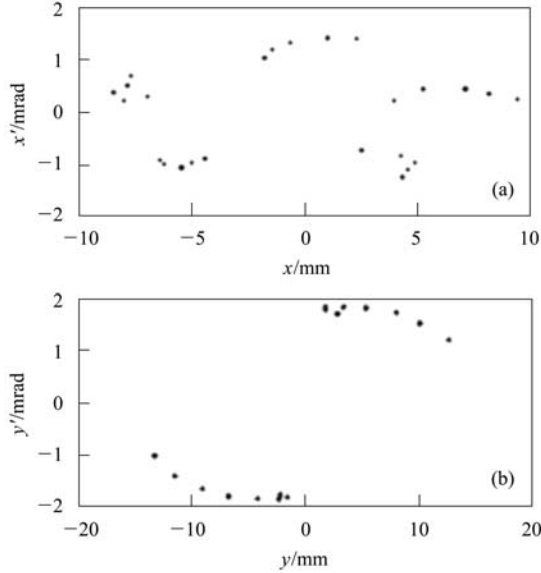

Fig. 10.   (a) The Poincaré map in the horizontal direction during 625-649 turns; (b) the poincaré map in the vertical direction during 637-652 turns of test particle E.

The simulation results show that a resonance becomes dominant in one stage in a cycle, and another resonance may be driven in another stage. Chaos motion appears in this procedure and some particles move to the outside of the beam core and become halo particles.

4   Space charge effects VS. tunes

In the simulations, to study the dependence of emittance growth on tunes, also two kinds of initial transverse distribution, KV distributions and painted distributions, are adopted. Tunes around the design values of 4.86/4.78 are compared. In simulations with initial KV distribution, strong coupling is observed and depends on the tunes. Fig. 11 shows that the normalized rms emittance exchange depends on the tunes. For the KV distribution, the emittance exchange disappears for $v_x - v_y > 0.12$ and $v_x = v_y$.
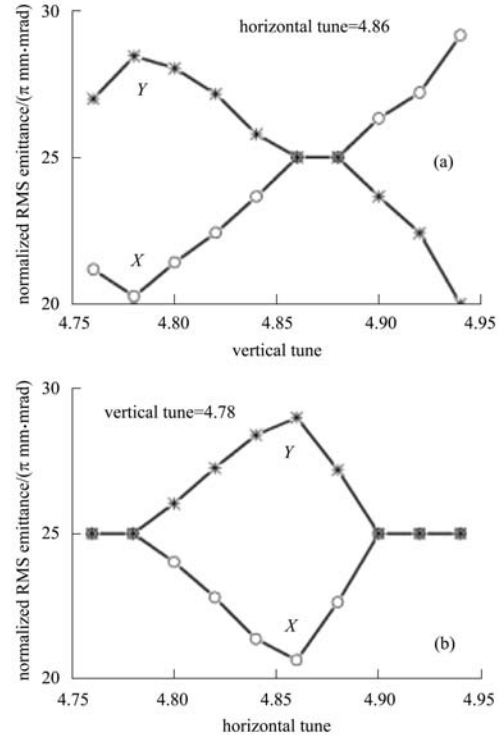

Fig. 11.   The dependence of coupling on tunes with initial KV distribution (a) for fixed v_x=4.86; (b) for fixed v_y=4.78.
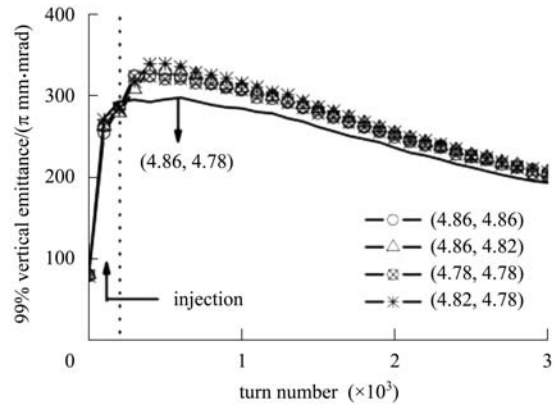

Fig. 12.   The time evolution of unnormalized 99% emittance during the early stage of acceleration for different tunes with initial real distribution.

Due to the fact that the Montague resonance is a different resonance, such coupling can lead to a significant effect for a nonequipartitioned beam. For the case of $\upsilon_x = \upsilon_y$, there is no emittance exchange, because the beam is equipartitioned.

As discussed in the "Space charge effects during acceleration" section, no high-order collective beam mode and great rms emittance exchange are observed

in the simulations with painted distribution. For the tunes close to m $(\upsilon_x-\upsilon_y)$=0, there is a large emittance (99%) growth in the vertical direction, as shown in Fig. 12. For these tunes, the resonance m$(\upsilon_x - \upsilon_y)$=0 may be excited for some particles, as shown in Fig. 13, and then results in the vertical C-S invariant growth. As a result, the emittance grows.
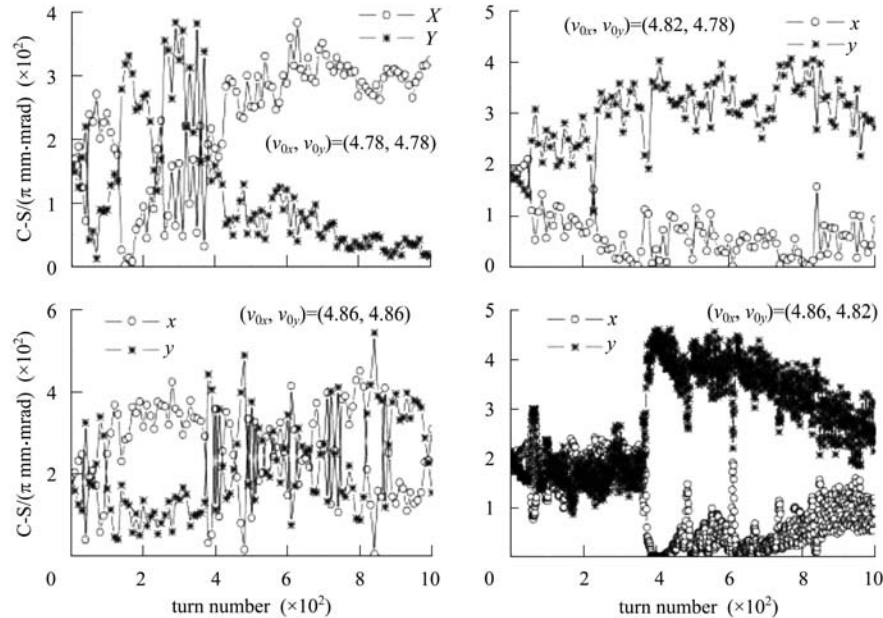

Fig. 13. The time evolution of the C-S invariant of some test particles for the tune of (4.78, 4.78), (4.82, 4.78), (4.86, 4.86), and (4.86, 4.82).

5 Conclusion

Space charge effects have been studied by simulation for the CSNS/RCS. Aiming at obtaining uniform painting distribution with space charge effects, a new bump function is derived and, based on this bump function, the painting distribution, which is very close to uniform distribution, is obtained. The space charge effects during the acceleration are studied and

the dangerous resonances which may induce emittance growth are investigated. The dependence of space charge effects on tunes is also simulated and analyzed. The results are an important reference for the design and commissioning of the CSNS/RCS.

References

1 WANG S et al. Chinese Physics C (HEP & NP), 2009, **33**(S2): 1–3
2 WEI J et al. Chinese Physics C (HEP & NP), 2009, **33**(11): 1033–1042
3 Machida S. The Simpsons Program User's Reference Manual, July. 1992
4 Galambos J D et al. ORBIT Use's Manual V.1.0, July. 1999
5 WANG J B, Fedotov A V, WEI J. Proceedings of the EPAC 2000, Vienna, Austria
6 TANG J Y, QIU J, WANG S, WEI J. HEP & NP, 2006, **30**(12): 1184–1189 (in Chinese)
7 QIU J, TANG J Y, WANG S, WEI J. HEP & NP, 2007, **31**(10): 942–946 (in Chinese)
8 Galambos J et al. Proceedings of the PAC'99, New York
9 WEI T, WANG S, QIU J, TANG J Y, QIN Q. Chinese Physics C (HEP & NP), 2010, **34**(2): 218–223
10 XU S Y. Ph. D. thesis. Graduate University of Chinese Academy of Sciences. 2011
11 Fedotov A V, Holmes J, Gluckstern R L. Phys. Rev. ST AB, 2001, **4**: 084202
12 Hofmann I, Frankenheim O B. Phys. Rev. Lett., 2001, **87**: 034802
13 Hofmann I. Phys. Rev. E, 1998, **57**: 4713
14 Montague B W. CERN Report, 68-38. 1968
15 Fedotov A V et al. Proceedings of the PAC'01, Chicago
16 Hofmann I, QIANG J, Ryne R D. Phys. Rev. Lett., 2001, **86**: 2313